INTERACTION BETWEEN PARTICLE CLUSTERS AND FLUID TURBULENCE

Takeo Kajishima
Department of Mechanical Engineering, Osaka University
Yamadaoka, Suita, Osaka, 565-0871 Japan
kajisima@mech.eng.osaka-u.ac.jp

Saotshi Takiguchi
Department of Mechanical Engineering, Osaka University
Current address: Mitsubishi Heavy Industries, Ltd.
Arai-cho, Takasago, 676-8686 Japan
takiguti@ws.trdc.mhi.co.jp

ABSTRACT

To investigate the two-way interaction between particles and fluid turbulence, a homogeneous flow field including solid particles was numerically simulated. Particular attention was focused on the clustering of particles, which might enhance turbulence, by energy supply through larger scale in comparison with dispersed particles. In the particle Reynolds number range from 50 to 400, it was found that particle clusters are formed by wake and vortex shedding enhances them. The Reynolds number dependence, dynamics and time scale of particle clusters are discussed in this paper.

INTRODUCTION

The objective of our research is to improve turbulence models and particle-tracking method for the unsteady simulation of particle-laden flows mainly by the large-eddy simulation (LES). With industrial and geophysical interests, we wish to expand the applicability of LES to flows including solid particles moving at relatively high Reynolds number, $Re_{ps} = \mathcal{O}[10^2]$ based on slip velocity and particle diameter.

Hereafter we consider the uni-scale sphere for solid particles. Even for the most fundamental case, in which a sphere is fixed in a uniform stream, the flow pattern changes drastically in the above-mentioned Reynolds number range as observed experimentally (Sakamoto and Haniu, 1990). Figure 1 shows typical examples of unsteady vortex shedding obtained by our method (Takiguchi et al., 1999; Kajishima et al., 1999) developed prior to this study. Reynolds number dependence of flow patterns as well as the time-averaged drag are in good agreement with experimental data.

As shown in Fig. 1, the unsteady vortex shedding takes place when Reynolds number Re_{ps} exceeds approximately 300. The orientation of shed vortices slightly alters at $Re_{ps} = 400$. The period and shape of vortices are getting more irregular for $Re_{ps} \geq 500$.

When the vortex shedding from solid particles takes place, turbulence energy induced through wake is not fully dissipated in the region near a particle. We estimated approximately 20% of particle work became an additional source of turbulence energy through vortex shedding (Kajishima, et al., 1999). However, uniformly distributed particles attenuated turbulence since wakes reduced the length-scale of background turbulence and modified it to more dissipative structure. On the other hand, turbulence was augmented when non-uniformity of particle distribution increases because turbulence energy was supplied at larger scale.

On the basis of above-mentioned observations, we proposed the particle Reynolds number and the inter-particle distance as important factors of particle effects on turbulence (Kajishima et al., 1999). To parameterize them, we must clarify the dynamics of particle clusters as well as its interaction with fluid turbulence.

The region with high concentration of particle is sometimes referred to as the cluster. Note that particles in the cluster do not always contact to each other. There have been some possible explanations for the mechanism of clustering: preferential concentration of par-

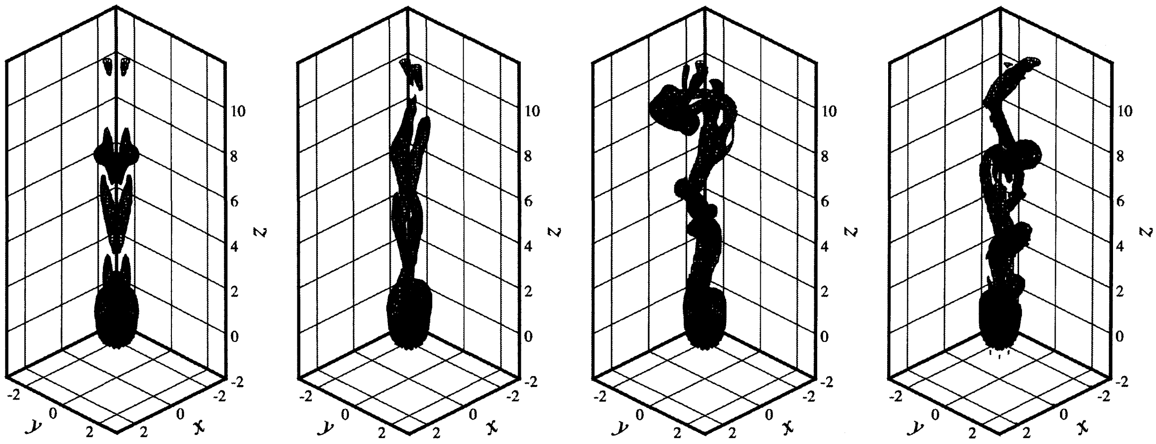

(a) $Re_{ps} = 300$ (b) $Re_{ps} = 400$ (c) $Re_{ps} = 500$ (d) $Re_{ps} = 600$

Figure 1: Unsteady vortex shedding from sphere particle fixed in a uniform stream: instantaneous vortex structures visualized by $\nabla^2 p$ iso-surfaces.

ticles in particular portion of turbulence eddies (realized numerically by Eaton and Fessler, 1994, for example), inelastic collision between particles (Goldhirsch and Zanetti, 1993, for example) and so on. The former is observed for small particles and the next is an inter-particle effect. Thus the two-way interaction between solid particles and fluid turbulence is not so important in these cases. However, the two-way interaction is essential in the Reynolds number range of our interest, $Re_{ps} = \mathcal{O}[10^2]$.

In this study, we investigate the dynamics of the wake-induced clusters of particles and the interaction between particles and fluid flow by means of direct numerical simulation (DNS) method.

OUTLINE OF COMPUTATION

To deal with this particular range of particle Reynolds number, we developed a two-way coupling scheme based on the finite-difference method (Takiguchi et al., 1999; Kajishima et al., 1999) for DNS. In our calculation, flows around a number of moving particles are directly resolved and the particle motion is governed by the surface integral of fluid stress together with body force such as gravity.

We derived a fortified Navier-Stokes equation for two-way coupling at the cell including solid-fluid boundary (Kajishima et al., 1999). The additional term at the boundary cell is

$$\boldsymbol{f}_p = \alpha\left(\boldsymbol{u}_p - \widehat{\boldsymbol{u}}\right)/\Delta t \tag{1}$$

where $\boldsymbol{u} = (1-\alpha)\boldsymbol{u}_f + \alpha\boldsymbol{u}_p$ is the volume-weighted average of velocity, α the volumetric fraction of solid, $\boldsymbol{u}_f$ the fluid velocity, $\boldsymbol{u}_p$ the velocity inside the solid particle ($\boldsymbol{u}_p = \boldsymbol{v}_p + \boldsymbol{r} \times \boldsymbol{\omega}_p$), $\boldsymbol{v}_p$ the particle velocity and $\boldsymbol{\omega}_p$ the angular velocity. It modifies $\widehat{\boldsymbol{u}}$ predicted using fluid flow equation to $\boldsymbol{u}$ after an advancement of time interval Δt. Using $\boldsymbol{f}_p$, the surface integral of fluid stress $\boldsymbol{\tau}$ in the equations for particle is replaced by the volumetric integral of $\boldsymbol{f}_p$ as

$$\begin{aligned} \int_{S_p} \boldsymbol{\tau}\cdot\boldsymbol{n}dS &= -\int_{V_p} \boldsymbol{f}_p dV\ , \\ \int_{S_p} \boldsymbol{r}\times(\boldsymbol{\tau}\cdot\boldsymbol{n})dS &= -\int_{V_p} \boldsymbol{r}\times\boldsymbol{f}_p dV\ . \end{aligned} \tag{2}$$

Since the grid for fluid flow is used for the volumetric integral, there is not residual in momentum exchange between two phases.

Hereafter in this study, we ignore the rotation of particles.

A major merit of our scheme is the applicability for wide range of particle Reynolds number, since it does not use any models for particle motion. In addition, it does not reduce numerical efficiency in comparison with previous method using point source models (Maxey and Riley, 1983; Elghobashi and Truesdell, 1992).

We apply our DNS method to a homogeneous turbulence including sphere particles. The computational setup is summarized in Table 1. Grid points for fluid turbulence simulation are distributed uniformly in a periodic computational domain. The number of grid points for fluid turbulence is 34 millions. The ratio of particle diameter to grid spacing is 10, which allowed enough accuracy for particle Reynolds number range with vortex shedding (Takiguchi et al., 1999; Kajishima et al., 1999). The number of particles is 128, corresponding to the volumetric fraction 0.2%. In such dilute addition, inter-particle collisions might

Table 1: Numerical setup for DNS of homogeneous flow including falling particles.

Number of grid points		
Horizontal	N_x, N_y	256×256
Vertical	N_z	512
Grid resolution for particle diameter		
	D_p/Δ	10
Properties of solid particles		
Number of solid particles	N_p	128
Density ratio	ρ_p/ρ_f	10
Reynolds number	Re_{ps}	50~400
Stokes number	St_p	27.8~222
Volmetric fraction	ε_p	0.20%
Mass loading ratio	ϕ_p	1.96%

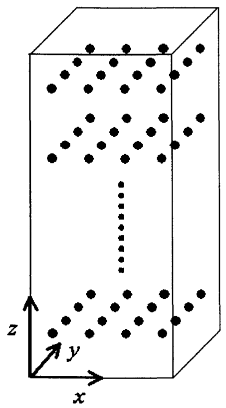

Figure 2: Coordinate and initial condition: fluid and particles are at rest.

not dominate the particle distribution and the flow field. The density of particle is assumed to be 10 times larger than that of fluid. So particles fall down by gravity. To keep the mass flow rate of the mixture to be zero, we supplemented the vertical gradient of pressure in the equation of fluid motion.

The Reynolds number is adjusted by changing the fluid viscosity so that the gravity and drag are in balance. The drag is estimated by the standard Re_{ps}-C_D curve for the fixed ball in a uniform flow (Clift, et al., 1978). The Reynolds number, Re_{pt}, based on the particle diameter and the terminal velocity of falling particle(s) in a periodic domain is different from settled Re_{ps}.

We simulated 4 cases, Re_{ps} =50, 100, 200 and 400. Initially, particles were disposed in order and particles and fluid were at rest, as shown in Fig. 2. The flow field was advanced in time to the fully developed stage.

RESULTS AND DISCUSSION

Figure 3 compares the time-averaged drag coefficients C_D. The average of C_D on particles should be compared with that on a particle in the same boundary condition, namely the pe-

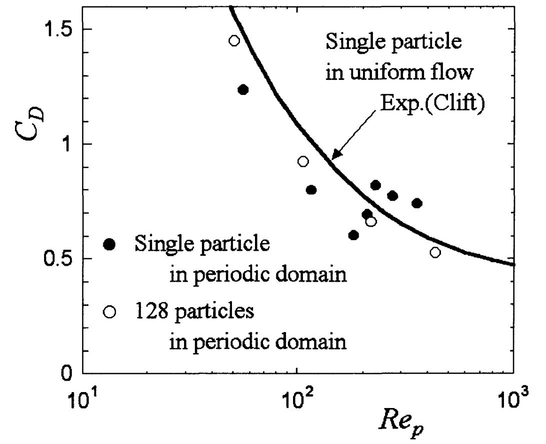

Figure 3: Drag coefficient on a sphere: comparison among single sphere fixed in uniform stream, single sphere in a periodic box, and falling spheres in a periodic box.

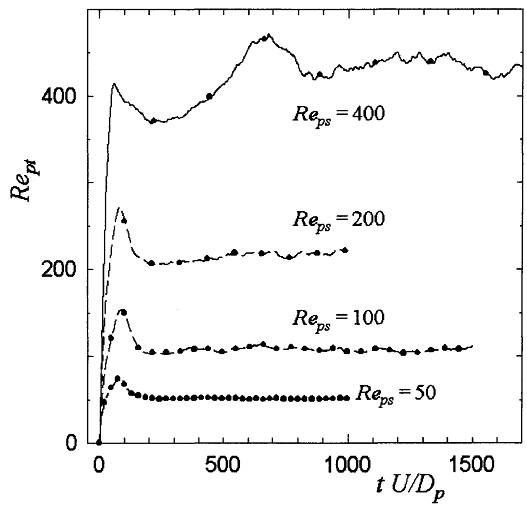

Figure 4: Time evolution of averaged Reynolds number of falling particles: plots are given at interval of particle response time.

riodicity assumption in every direction. The drag on a particle in a periodic box, which is identical to one of particles in array, differs from that on a particle in a uniform stream because of the influence of wakes of upstream ones. In low Reynolds number range, the drag is reduced due to smaller velocity in the wake. In high Reynolds number range, on the other hand, the drag is increased due to the fluctuation of the wake. Thus the drag coefficient profile for a sphere particle in a periodic domain jumps at around Re_{pt} = 200 ~ 300.

The drag on particles trapped in the wake of upstream ones could be smaller than those falling individually. Thus they approached ones in lower position. This is the mechanism of clustering due to vortex shedding in the wake. Since particles tend to form clusters in

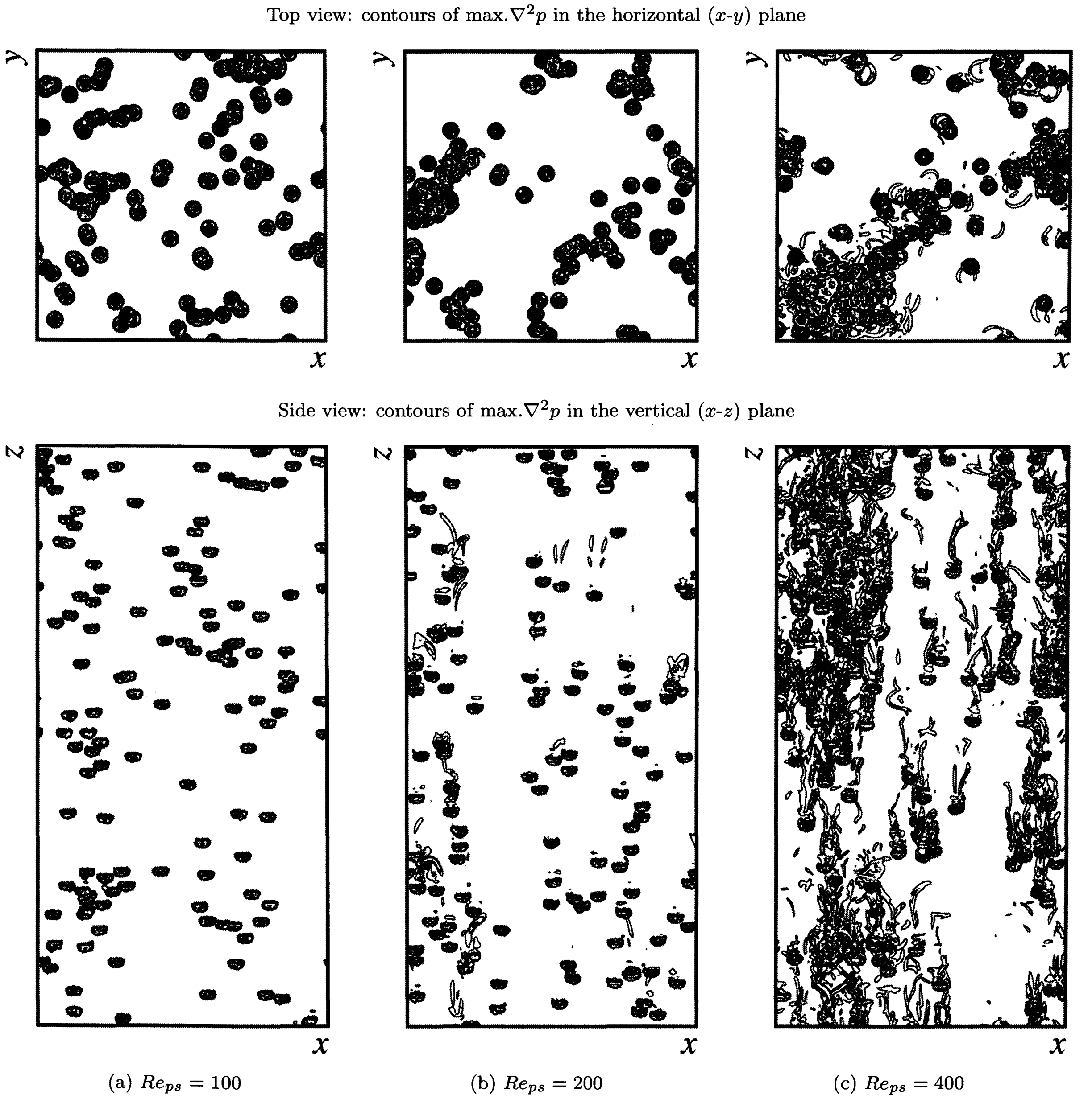

Figure 5: Instantaneous flow field, including 128 particles falling down, visualized by $\nabla^2 p$ projected in the horizontal and vertical planes.

higher Reynolds number range, C_D decreases in comparison with that for a single particle as shown in Fig. 3.

The decrease in C_D of particles results in the increase in average Re_{pt} as shown in Fig. 4. For higher Re_{ps}, Re_{pt} of falling particles increase from Re_{ps}, and it fluctuates with time. Particles of lower Reynolds numbers such as Re_{ps} =50 and 100, on the other hand, fall down with constant velocity.

Figure 5 shows instantaneous flow field including particles. Particles of Re_{ps} =100 are dispersed. On the contrary, particles of Re_{ps} =400 form strong clusters as represented by high-density region in Fig. 5(c). As for the Reynolds number range in between them, single particle with Re_{ps} =200 does not shed vortices. But the particles form small clusters as shown in Fig. 5(b) and some of them shed vortices similarly to a particle with higher Reynolds number.

We guess the monotonous decrease in C_D shown in Fig. 3 is the consequence of continuous increase in size and/or number of clusters with Re_{ps} increase as shown in Fig. 5.

Figure 6 shows the three-dimensional spectrum of horizontal velocity fluctuation u'_f (and v'_f). With increase in Re_{ps}, the energy increases firstly in low wave-number range and then in higher wave-number range. The former is due to the increase in non-uniformity of

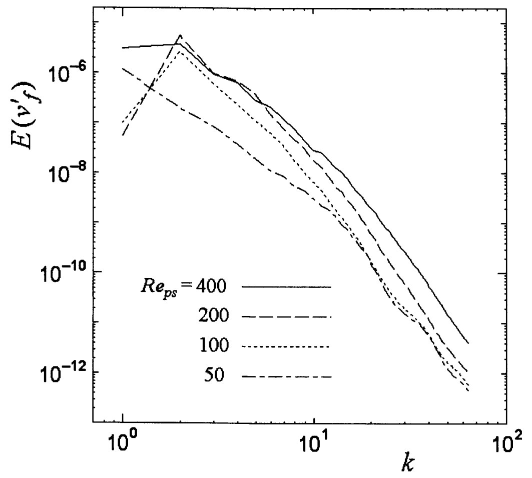

Figure 6: Three-dimensional spectrum of horizontal velocity fluctuations.

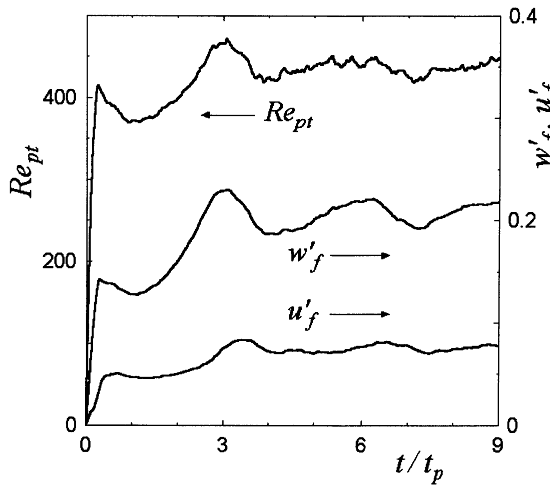

Figure 7: Time evolutions of mean particle Reynolds number and turbulence intensities in vertical and horizontal directions ($Re_{ps} = 400$).

particle distribution and the latter is due to the vortex shedding. In addition, for $Re_{ps} = 400$, the energy at the smallest wave-number end in our computational domain still grows due to growing cluster.

Figure 8 shows top views of particle distribution for every particle response time t_p in the case of $Re_{ps} = 400$. Clusters grow in size, move and break up. Our computational domain is enough for the observation of particle clusters but it seems somewhat small for cluster-cluster or cluster-turbulence interactions.

To consider the life cycle of particle clusters, relationship between particle motion and Reynolds stress components are shown in Fig. 7. Due to smaller drag on particles in the cluster, they fall faster than the terminal velocity of single particle. So we can detect the cluster by the particle Reynolds number Re_{ps}. At $t = 3t_p$, the maximum of Re_{pt} shown in Fig. 7 is due to 4 small clusters observed in Fig. 8. Then they are re-arranged to larger ones.

A cluster causes downward current of fluid moving with it. As shown in Fig. 7, the vertical fluctuation of fluid velocity w'_f synchronizes with Re_{ps} and the horizontal component u'_f also does with slight delay (maybe after the redistribution among components of velocity fluctuation). The turbulence shear stress is consequently intensified and resists the cluster motion, resulting in break-up of cluster. This is a life cycle of particle cluster in the homogeneous fluid flow.

Spatial and temporal scales of clusters may depend on particle response time t_p, particle loading ratio ε_p and the background turbulence. In our particular case without extra source of turbulence other than the existence of particles, the period from clustering to break-up is supposed to be several times of t_p as shown in Fig. 7. But a series of computation is required to parameterize the cluster dynamics for wider range of conditions.

Conclusions

The direct numerical simulation reproduced the cluster, the high concentration region, of solid particles in homogeneous turbulence. Since clusters were caused by wakes from particles in our case, a scheme to resolve flows around all particles was essential. Clusters grows with particle Reynolds number, especially in the case particle Reynolds number exceeds 300. Particle cluster induced large scale eddies into the fluid flow and finally broke up due to the turbulence stress generated around it. The period from growing to break-up seemed to be a function of particle response time for the case without background turbulence.

Our result suggests the turbulence energy induced through particle wakes, the scale of particles clusters and the Reynolds number dependence of them are important factors to improve turbulence models for particle-laden fluid flow.

References

Clift, R., Grace, J. R. and Weber, M. E., 1978, "Bubbles, drops, and particles", Academic Press, New York.

Eaton, J. K. and Fessler, J. R., 1994, "Preferential concentration of particles by turbu-

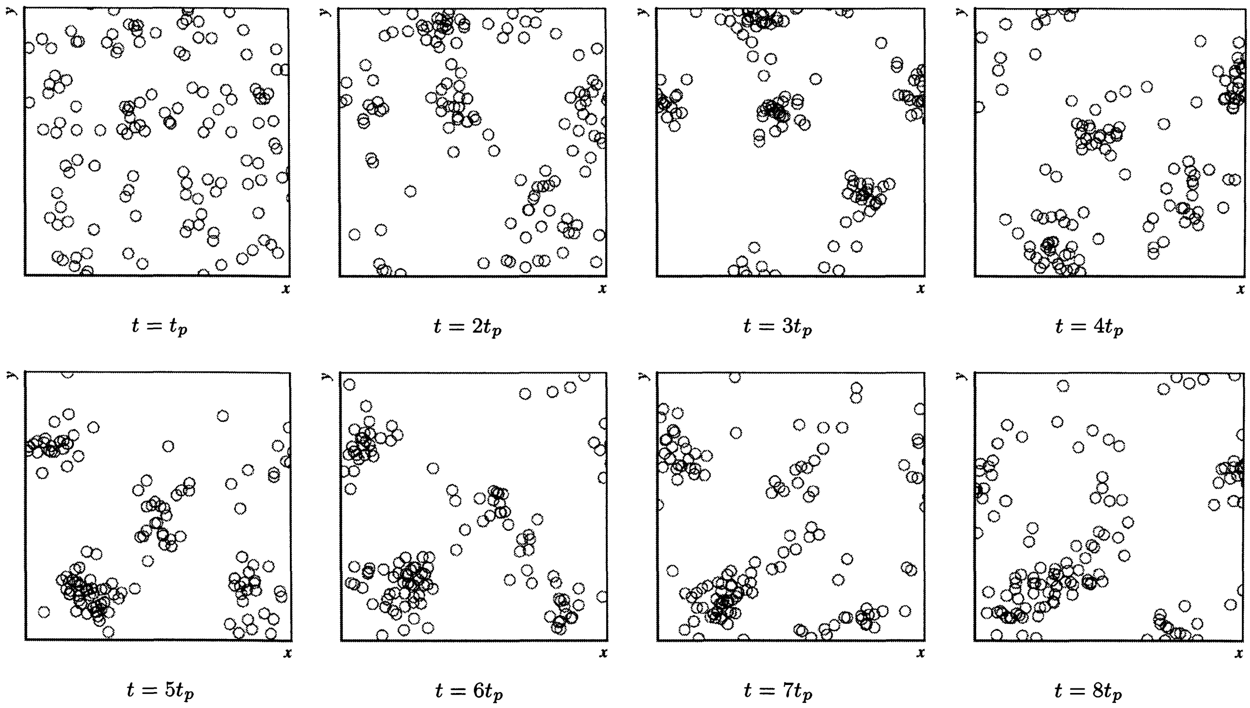

Figure 8: Time evolution of particle distribution ($Re_{ps} = 400$).

lence", Int. J. Multiphase Flow, Vol.20 suppl., pp.169-209.

Elghobashi, S. and Truesdell, G. C., 1992, "Direct simulation of particle dispersion in a decaying isotropic turbulence", J. Fluid Mech., Vol.242, pp.655-700.

Goldhirsch, I. and Zanetti, A., 1993, "Clustering instability in dissipative gases", Phys. Rev. Letters, Vol.70, No.11, pp.1619-1622.

Kajishima, T., Takiguchi, S. and Miyake, Y., 1999, "Modulation and subgrid scale modeling of gas-particle turbulent flow", Recent Advances in DNS and LES (Eds. Knight,D. and Sakell,L.), Kluwer Academic, pp.235-244.

Maxey, M. R. and Riley, J. J, 1983, "Equation of motion for a small rigid sphere in a nonuniform flow", Phys. Fluids, Vol.26, No.4, pp.883-889.

Sakamoto, H. and Haniu, H., 1990, "A study on vortex shedding from spheres in a uniform flow", Trans. ASME, J. Fluids Eng., Vol.112, pp.386-392.

Takiguchi, S., Kajishima, T. and Miyake, Y., 1999, "Numerical scheme to resolve the interaction between solid-particles and fluid-turbulence", JSME Int. J., Ser.B, Vol.42, No.3, pp.411-418.